A Machine Learning-Based Pulse Detection Algorithm for Use During Cardiopulmonary Resuscitation

Iraia Isasi[1], Erik Alonso[1], Unai Irusta[1], Elisabete Aramendi[1], Morteza Zabihi[2], Ali Bahrami Rad[3], Trygve Eftestøl[4], Jo Kramer-Johansen[5], Lars Wik[5]

[1] University of the Basque Country (UPV/EHU), Bilbao, Spain
[2] Massachusetts General Hospital, Boston, United States
[3] Emory University, Atlanta, United States
[4] University of Stavanger, Stavanger, Norway
[5] Oslo University Hospital, Oslo, Norway

Abstract

Resuscitation guidelines mandate pausing chest compressions (CCs) during cardiopulmonary resuscitation (CPR) to check for the presence of pulse. However, interrupting CPR during a pulseless rhythm adversely affects survival. The aim of this study was to develop a pulse detection algorithm during CPR using the ECG and thoracic impedance (TI) signals. Data were collected from 116 out-of-hospital cardiac arrest (OHCA) patients during CCs and pulse/no-pulse annotations were carried out in artefact-free intervals by clinicians. CC artefacts were first removed from ECG and TI using recursive least-squares (RLS) filters. The impedance circulation component (ICC) was then derived from the filtered TI using a RLS-based adaptive scheme. The wavelet decomposition of the ECG and ICC was carried out to obtain the different subband components and the reconstruced ECG and ICC. A total of 124 discrimination features were extracted from those signals and fed into a random forest (RF) classifier that made the pulse/no-pulse decision. A repeated cross-validation procedure was used for feature selection, parameter tuning, and model assessment. Pulse/no-pulse diagnoses obtained through the RF were compared with the annotations to obtain the sensitivity (SE), specificity (SP) and balanced accuracy (BAC) of the method. The results obtained were: 76.2% (SE), 66.2% (SP) and 71.2% (BAC).

1. Introduction

Out of hospital cardiac arrest (OHCA) is a leading cause of death in the industrialized world, with an estimated annual average incidence of 83.7-95.9 per 100.000 person-years and low survival rates of around 10% [1]. The detection of pulse is crucial for the recognition of the cardiac arrest and the return of spontaneous circulation (ROSC) [2].

A rapid recognition of cardiac arrest allows for a prompt initiation of cardiopulmonary resuscitation (CPR) and an early defibrillation, whereas a rapid identification of ROSC leads to an immediate initiation of post-resuscitation care.

In OHCA, pulse detection consists in the discrimination of two types of organized rhythms, i.e rhythms presenting visible QRS complexes in the ECG: pulseless electrical activity (PEA) and pulse-generating rhythm (PR). During PR both normal electrical (QRS complexes) and mechanical activity (contraction of the myocardium) of the heart are present, whereas PEA is characterized by the dissociation between the mechanical and electrical activities, which leads to no palpable pulse. Although PR often shows more regular and narrower QRS complexes than PEA, the differences between both rhythms are not always detectable in the ECG. In such cases, the thoracic impedance signal (TI) can help discriminate PEA and PR as it shows an impedance circulation component (ICC) consisting in small fluctuations (< 100 mΩ) correlated with the QRS complexes for PR, but not for PEA.

Several signal processing and machine/deep learning algorithms have been developed in the literature for the detection of pulse based solely on the ECG [3] or the thoracic impedance (TI) signals [4], or on the combination of the ECG and TI [5]. All these algorithms were designed to work during pauses in chest compressions (CCs). Unfortunately, artefacts introduced by the mechanical activity of CCs during CPR make those pulse detection algorithms unreliable. Therefore, CPR must be interrupted for a reliable pulse detection analysis, adversely affecting OHCA survival.

The aim of this study was to develop an algorithm that detects pulse during CPR using the ECG and TI signals. This solution would allow pulse detection during CPR eliminating the no-flow intervals for rhythm analysis and contributing to improve OHCA survival rates.

2. Materials and methods

2.1. Dataset

The data were obtained from a prospective study of out-of-hospital cardiac arrest (OHCA) patients gathered between March 2002 and September 2004 by the emergency services of London, Stockholm and Akershus [6]. The ECG, the compression depth (CD) and the thoracic impedance (TI) signals were acquired using a modified version of Laerdal's Heartstart 4000 defibrillator (4000SP) and were resampled to 250 Hz. Chest compressions time instants (t_k) were automatically marked in the CD signal using a negative peak detector for depths above 1 cm.

The dataset used in this study contained 429 records obtained from 116 OHCA patients. Each record was composed of concurrent ECG and TI segments consisting of two consecutive intervals (see Figure 1): a 12.5 s interval which includes continuous CCs, and a 3 s interval free of artefacts. The interval during CCs was used to develop the pulse detection algorithm whereas the interval free of artefacts was reviewed by expert resuscitation rhythm reviewers to annotate the patient's underlying rhythm as PEA/PR. In total there were 290 PEA and 139 PR.

2.2. Filtering the CPR artefact

The CPR artefact was modeled both in the corrupt TI, $s_{\text{corTI}}(n)$, and the corrupt ECG signal, $s_{\text{corECG}}(n)$, as a quasi-periodic interference using a Fourier series truncated to N harmonics and locked to the fundamental frequency of the CCs, $f_0(n)$ [7]:

$$s_{\text{cpr}}(n) = \sum_{k=1}^{N} a_k(n)\cos(k2\pi f_0(n)nT_s)+ \tag{1}$$
$$b_k(n)\sin(k2\pi f_0(n)nT_s)$$

$$f_0(n) = \frac{1}{t_k - t_{k-1}} \quad t_{k-1} < nT_s \leq t_k \tag{2}$$

The time-varying in-phase, $a_k(n)$, and quadrature, $b_k(n)$, coefficients were adaptively estimated using the recursive least squares (RLS) algorithm to minimize the error between the corrupt signal (ECG or TI) and the estimated artefact at the harmonics of $f_0(n)$. We will denote as $\hat{s}_{\text{cprECG}}(n)$ and $\hat{s}_{\text{cprTI}}(n)$ the artefacts estimated in the corrupt ECG and TI signals, respectively. The filtered ECG, $\hat{s}_{\text{ECG}}(n)$ and TI, $\hat{s}_{\text{TI}}(n)$, signals were then obtained by substraction:

$$\hat{s}_{\text{ECG}}(n) = \hat{s}_{\text{corECG}}(n) - \hat{s}_{\text{cprECG}}(n) \tag{3}$$
$$\hat{s}_{\text{TI}}(n) = \hat{s}_{\text{corTI}}(n) - \hat{s}_{\text{cprTI}}(n) \tag{4}$$

2.3. Extraction of the ICC

The ICC was estimated from the filtered TI signal, $\hat{s}_{\text{TI}}(n)$, using the same RLS-based adaptive scheme as the
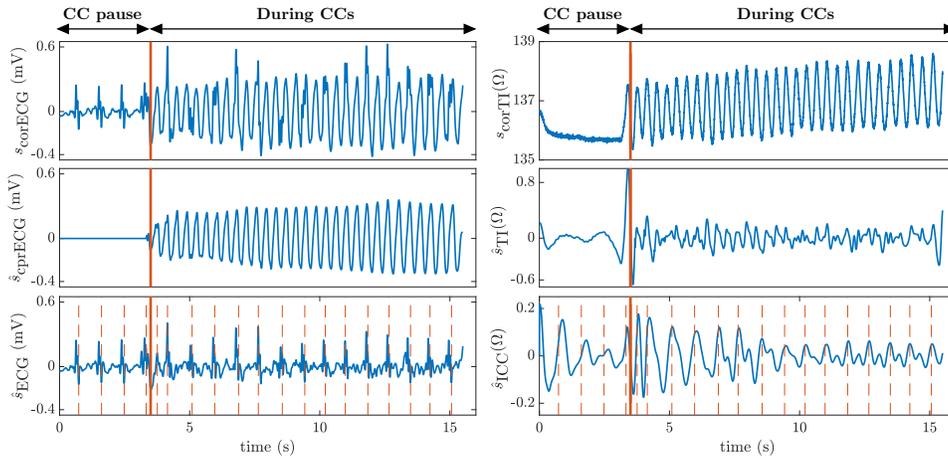

Figure 1. An example of a dataset segment corresponding to a patient with pulse (PR). The left panel shows the signals derived from the corrupted ECG signal, from top to bottom: the corrupted ECG, $s_{\text{corECG}}(n)$, the estimated CPR artefact, $\hat{s}_{\text{cprECG}}(n)$, and the filtered ECG, $\hat{s}_{\text{ECG}}(n)$. In the first 3 s there is no artefact and the underlying PR is visible. Filtering, $\hat{s}_{\text{ECG}}(n)$, reveals the underlying rhythm of the patient in the 12.5 s artefacted interval. The right panel shows the signals derived from the corrupted TI signal, from top to bottom: the corrupted TI, $\hat{s}_{\text{corTI}}(n)$, the filtered TI, $\hat{s}_{\text{TI}}(n)$ and the ICC, $\hat{s}_{\text{ICC}}(n)$. The QRS complex instants are highlighted using vertical dashed red lines both in the $\hat{s}_{\text{ECG}}(n)$ and $\hat{s}_{\text{ICC}}(n)$ to show the correlation between both signals during CPR.

one used in the previous section [5]. As the CPR artefact, the ICC was modeled in $\hat{s}_{TI}(n)$ as a quasi-periodic interference (Eq.1), but in this case the Fourier series was locked to the fundamental frequency, $f_c(n)$, of the QRS complexes. The QRS complex instants required for the calculation of $f_c(n)$ (Eq. 2) were obtained using the Hamilton-Tompkins algorithm on the filtered ECG [8]. Finally, the time-varying a_k and b_k coefficients of the Fourier series model (Eq 1.) were adaptively estimated to minimize the error between the filtered TI signal, $\hat{s}_{TI}(n)$, and the estimated ICC, $\hat{s}_{ICC}(n)$, at the harmonics of $f_c(n)$.

3.   Feature engineering

A multi-resolution analysis based on the stationary wavelet transform (SWT) was employed to extract 124 PEA/PR discrimination features, 93 derived from the filtered ECG, $\hat{s}_{ECG}(n)$, and 31 from the ICC, $\hat{s}_{ICC}(n)$. Only the interval from 4 s to 12 s of both the filtered ECG and ICC segments was used to compute features. First 4 s were left out to avoid RLS filtering transients. The 8 s $\hat{s}_{ECG}(n)$ and $\hat{s}_{ICC}(n)$ segments were decomposed by SWT into its subbands with the Daubechies 4 wavelet and 8 levels of decomposition generating an approximation coefficient a_8 and 8 detail coefficients d_1 to d_8. The filtered ECG, $\hat{s}_{ECG}(n)$, was then reconstructed, $\hat{s}_{recECG}(n)$, by using detail coefficients $d_3 - d_7$ (0.98-31.25 Hz band). Detail coefficients $d_6 - d_8$ (0.49-3.91 Hz band) for heat rates above 117 bpm, $d_7 - d_8$ (0.49-1.95 Hz band) for heart rates between 58 and 117 bpm or simply d_8 (0.49-0.98 Hz band) for segments with heart rates below 58 bpm were used to reconstruct the ICC, $\hat{s}_{recICC}(n)$.

The 93 features corresponding to the ECG were extracted from the reconstructed ECG, $\hat{s}_{recECG}(n)$, and $d_3 - d_7$ detail coefficients. These parameters are the same as those implemented by Isasi et al. [7] for OHCA multiclass rhythm classification, so their detailed description can be found at [7].

The 31 features corresponding to the ICC, were computed from $\hat{s}_{ICC}(n)$, its first derivative $\hat{s}_{dICC}(n)$, and its $d_5 - d_8$ detail coefficients. The first 6 features were the mean peak-to-through amplitude (MPT), the standard deviation of the mean peak-to-through amplitude (SDPT), and the mean area (MA) of $\hat{s}_{ICC}(n)$ and $\hat{s}_{dICC}(n)$. The following 24 features were the fuzzy entropy (FuzzyEn), the skewness (Skew), the kurtosis (Kurt) and the interquartile ranges (IQR) of $\hat{s}_{ICC}(n)$, $\hat{s}_{dICC}(n)$ and $d_5 - d_8$. Finally, the mean cross power between $\hat{s}_{ICC}(n)$ and $\hat{s}_{recECG}(n)$ was computed. A more detailed description of these features can be found at [5].

4.   Classifier

The last step in the pulse detection algorithm is classification. Random forest (RF) classifiers were used to classify the rhythm as PEA/PR. A repeated 5-fold cross-validation (CV) architecture was used for feature selection, hyperparameter optimization and model assessment. First, for each training set of the 5-fold CV, $K = 20$ features were selected using recursive feature elimination (RFE) [7]. Then, each training set of the 5-fold CV loop, was further split into training (75%)/test (25%) to select the optimal hyperparameters of the RF. Once the optimal features and parameters were selected, the classifier was trained and assessed in the 5-fold CV loop. Data were always partitioned patient-wise and maintaining at least 90% of the PEA and PR proportions of the original dataset.

The model was evaluated in terms of sensitivity (SE, capacity to correctly detect PR), specificity (SP, capacity to correctly detect PEA) and balanced accuracy (BAC, mean of SE and SP). The performance metrics were calculated always in the test folds of the 5-fold CV loop by comparing the model's PR/PEA decisions with the ground truth labels set by expert reviewers. The PEA and PR class imbalance was addressed by assigning uniform prior probabilities for each class.

The minimum number of observations per leaf (l_{size}), which controls the depth of the trees, was the only RF hyperparameter optimized by doing a grid search in the range $1 \leq l_{size} \leq 200$. The number of trees in the forest was fixed to 300 and the number of features per split was set to the default value $\sqrt{K}$.

Feature selection was based on a RFE approach using the permutation importance of the RF as ranking criterion. At each iteration of the RFE algorithm features were ranked, and the least important 3% of the features were removed. The process was continued until $K = 20$ features were left for classification.

The 5-fold CV procedure was repeated 50 times using different random partitions to estimate the statistical distributions of the performance metrics and to avoid data partition bias. All the results are given as mean (SD) of the values obtained in the 50 repetitions of the experiments.

5.   Results

Table 1 shows the SE/SP and BAC values obtained with the proposed model, compared to the values obtained using a model based exclusively on ECG-features and a model trained using artefact-free intervals (see the first 3.5 s on Figure 1). The BAC obtained with the proposed model during CCs was only 4 points lower than that obtained during artefact-free intervals. Furthermore, adding TI features to the model based only on the ECG yielded a BAC improvement of 0.7%.
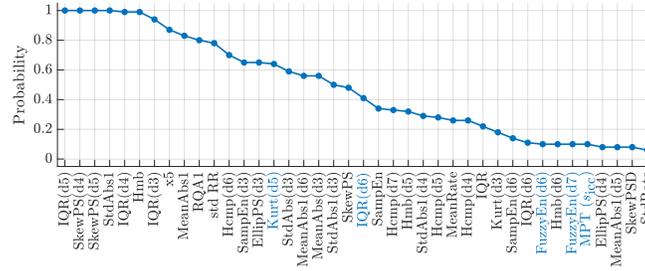
Figure 2. Selection probability for the 40 most selected features in the 250 runs of feature selection.

Table 1. Accuracy for a model trained using clean intervals, a model based exclusively on the ECG and the proposed model.

	Clean	ECG	ECG+TI
SE	78.2 (3.1)	77.3 (3.4)	**76.2 (3.0)**
SP	72.0 (2.8)	63.8 (2.8)	**66.2 (3.4)**
BAC	75.1 (1.6)	70.5 (1.6)	**71.2 (1.7)**

Figure 2 shows the 40 features with the highest probability of selection (the nomenclature of the features follows that of the original papers [5, 7]). These probabilities were estimated by counting the number of times the features were selected in the 250 runs of feature selection algorithm (50 repetitions of 5-fold CV). The features highlighted in blue correspond to the TI signal while the rest are derived from the ECG signal.

5.1. Conclusion

This work introduces a new method for pulse detection during CCs. It consists of adaptive filters for the removal of chest compression artefacts and the extraction of the ICC component, the multi-resolution analysis of the filtered ECG and ICC through the SWT and a RF classifier using features derived from the filtered ECG and the ICC that encompass the collective knowledge of active research in the field.

The results showed that the algorithm provided acceptable values for an accurate pulse detection during CCs as it obtained a BAC just 4 points lower than the one obtained by training the model using artefact-free intervals. As Figure 2 shows, the most selected features by the RF classifier were those derived from the ECG signal. However, the addition of the TI features to a model based exclusively on ECG features help improve the BAC by 0.7 points.

In conclusion, a novel algorithm based solely on the ECG or on the combination of the ECG and TI showed potential to improve resuscitation by reliably detecting pulse during CPR.

References

[1] J. Berdowski, R. A. Berg, J. G. Tijssen, and R. W. Koster, "Global incidences of out-of-hospital cardiac arrest and survival rates: systematic review of 67 prospective studies," *Resuscitation*, vol. 81, no. 11, pp. 1479–1487, 2010.

[2] J. Soar, J. P. Nolan, B. W. Böttiger, G. D. Perkins, C. Lott, P. Carli, T. Pellis, C. Sandroni, M. B. Skrifvars, G. B. Smith *et al.*, "European resuscitation council guidelines for resuscitation 2015: section 3. adult advanced life support," *Resuscitation*, vol. 95, pp. 100–147, 2015.

[3] A. Elola, E. Aramendi, U. Irusta, A. Picón, E. Alonso, P. Owens, and A. Idris, "Deep neural networks for ecg-based pulse detection during out-of-hospital cardiac arrest," *Entropy*, vol. 21, no. 3, p. 305, 2019.

[4] J. Ruiz, E. Alonso, E. Aramendi, J. Kramer-Johansen, T. Eftestøl, U. Ayala, and D. González-Otero, "Reliable extraction of the circulation component in the thoracic impedance measured by defibrillation pads," *Resuscitation*, vol. 84, no. 10, pp. 1345–1352, 2013.

[5] E. Alonso, U. Irusta, E. Aramendi, and M. R. Daya, "A machine learning framework for pulse detection during out-of-hospital cardiac arrest," *IEEE Access*, vol. 8, pp. 161 031–161 041, 2020.

[6] L. Wik, J. Kramer-Johansen, H. Myklebust, H. Sørebø, L. Svensson, B. Fellows, and P. A. Steen, "Quality of cardiopulmonary resuscitation during out-of-hospital cardiac arrest," *JAMA*, vol. 293, no. 3, pp. 299–304, 2005.

[7] I. Isasi, U. Irusta, A. B. Rad, E. Aramendi, M. Zabihi, T. Eftestøl, J. Kramer-Johansen, and L. Wik, "Automatic cardiac rhythm classification with concurrent manual chest compressions," *IEEE Access*, vol. 7, pp. 115 147–115 159, 2019.

[8] J. Pan and W. J. Tompkins, "A real-time QRS detection algorithm," *IEEE transactions on biomedical engineering*, no. 3, pp. 230–236, 1985.

Address for correspondence:

Iraia Isasi Liñero
Plaza Ingeniero Torres Quevedo 1, 48013 Bilbao, Spain
iraia.isasi@ehu.eus